

FSU-SCRI-99-71

HUB-EP-99/57

MPI-PhT/99-50

Two Loop Computation of the Schrödinger Functional in Lattice QCD



Achim Bode

SCRI, Florida State University
Tallahassee, Fl 32306-4130, USA

Peter Weisz

Max-Planck-Institut für Physik
Föhringerring 6, D-80805 München, Germany

Ulli Wolff

Institut für Physik, Humboldt Universität
Invalidenstr. 110, D-10099 Berlin, Germany

Abstract

We compute the Schrödinger functional (SF) for the case of lattice QCD with Wilson fermions (with and without SW improvement) at two-loop order in lattice perturbation theory. This allows us to extract the three-loop β -function in the SF-scheme. These results are required to compute the running coupling, the Λ -parameter and quark masses by finite size techniques with negligible *systematic* errors. In addition our results enable the implementation of two-loop $O(a)$ improvement in SF-simulations. This article is based on the revised version of ref.[11].

1 Introduction

Physical amplitudes in quantum chromodynamics (QCD) obey renormalization group equations whose solutions at high energy can be computed (in various leading logarithmic approximations) using renormalized perturbation theory. The solutions involve renormalization group invariant mass parameters, the so-called (scheme dependent) Λ parameter and the renormalization group invariant quark masses M . The determination of the relationships of these quantities to the low-lying hadron masses is a non-perturbative problem. For the quark masses there are various non-perturbative approaches including chiral perturbation theory, but the most systematic approach and the only one available for computing e.g. the ratio $\Lambda/M_{\text{proton}}$ is to employ the lattice regularization. There is already a vast literature on this subject (see e.g. the reviews [1]-[3]).

Among the collaborations which have as one of their main goals the computation of these relationships to as high precision as presently possible is the Alpha Collaboration. The collaboration's results in the quenched approximation have already been presented, most recently in [4]. The extension of the project to full QCD is now under way but due to the enormous extra cost in CPU time, without the sufficient compensation of computer power it will still take some time [5] until one can match the accuracy attained in the quenched approximation.

The emphasis of the Alpha project is on precision and directly associated with this, an attempt to carefully control systematic errors. The aim is to compute non-perturbatively defined running couplings and quark masses over a wide range of energies ranging from low energies where contact with hadronic mass parameters is made. To make contact with perturbation theory it is essential that the simulation reaches a range of high energy where the predicted behavior actually appears to set in. Our tactic to reach this goal has been explained in many publications [7], [8] and we refer the reader to these papers for further technical details. The key idea is to define a coupling $g(L)$ in a system with finite linear extension L (with specified boundary conditions). Adjusting a/L and the bare coupling so that $g(L)$ is kept fixed, the approach to the continuum limit of the coupling at twice the extension $g(2L)$ depends only on a/L . As a working hypothesis this approach is fitted by a power law (up to logarithmic factors) as expected from the Symanzik effective action analysis [1].

A specific such coupling $\alpha_{\text{SF}} = \bar{g}_{\text{SF}}/4\pi$, measured by the Alpha Collab-

oration is not directly experimentally accessible, but it can be related to phenomenological running couplings e.g. the $\overline{\text{MS}}$ coupling of dimensional regularization defined in infinite volume at high energies, using renormalized perturbation theory:

$$\alpha_{\overline{\text{MS}}}(sq) = \alpha_{\text{SF}}(q) + c_1(s)\alpha_{\text{SF}}(q)^2 + c_2(s)\alpha_{\text{SF}}(q)^3 + \dots \quad (1.1)$$

To reduce the estimated systematic errors introduced by truncation of the perturbative series to the level of $\sim 1\%$ it is necessary to work out this connection to two-loop order. For technical reasons this is at present accomplished in two steps. The first step, the computation of the relationship of $\alpha_{\overline{\text{MS}}}$ to the bare lattice coupling α_0 , has been completed in refs. [9],[10] and [11]. In this paper we perform the second step, the relationship of α_{SF} to α_0 for $N_f > 0$ flavors (the case $N_f = 0$ has already been presented in [12]-[14]).

The final result between the continuum quantities (1.1) is of course regularization independent, but the intermediate relations in both steps depend on the details of the lattice action employed. In our simulations we attempt to reduce lattice artifacts in the continuum limit by working with the Symanzik $O(a)$ -improved fermion action of Sheikholeslami and Wohlert [15]. The cancellation of extra $O(a)$ effects due to the presence of boundaries requires the introduction of additional boundary terms in the action. The weights of these terms can also be computed in perturbation theory and the computation presented here fixes the one relevant for the boundary conditions under consideration to two-loop order.

After recalling the definition of α_{SF} in the next section we will present some technical details, describing the Feynman diagrams involved in section 3. In section 4 we discuss the dependence of the perturbative coefficients on the lattice cutoff, and the related task of determining the boundary improvement coefficients mentioned above. In the final section 5 we compute the coefficients in eq.(1.1). A summary of part of this work has already been given in [16].

2 Basic definitions

The Schrödinger functional [7] is the QCD partition function

$$\mathcal{Z} = e^{-\Gamma} = \int D[U]D[\bar{\psi}]D[\psi]e^{-S}, \quad (2.1)$$

with the following particular geometry. In the spatial directions we have a finite box of size L (in all directions) with periodic-like boundary conditions (see below). The extent of the time (x_0) direction is also finite, T , and at the boundaries $x_0 = 0, x_0 = T$, Dirichlet boundary conditions (specified below) are imposed. The ratio T/L belongs to the definition of the SF and in this work we always restrict ourselves to the choice $T = L$.

The SF can be straightforwardly defined non-perturbatively by using the lattice regularization. In eq.(2.1) the links interior to the box are integrated over with the invariant $SU(3)$ measure, and the dynamical Grassmann fields $\psi(x), \bar{\psi}(x)$ are those at points x with $0 < x_0 < L$.

The action is taken to be

$$S[U, \bar{\psi}, \psi] = S[U] + S_W[U, \bar{\psi}, \psi] + S_{SW}[U, \bar{\psi}, \psi]. \quad (2.2)$$

The pure gauge part is defined by the usual sum over oriented plaquettes,

$$S(U) = \frac{1}{g_0^2} \sum_p w(p) \text{tr}(1 - U_p). \quad (2.3)$$

The weight $w(p)$ is unity for all plaquettes except those at the boundary that contain the time-direction and one of the frozen spatial links where we put

$$w(p) = c_t(g_0). \quad (2.4)$$

S_W has the form of the standard Wilson fermion action with $r = 1$,

$$S_W[U, \bar{\psi}, \psi] = \sum_{x, 0 < x_0 < L-1} \bar{\psi}(x) (D + M_0(x)) \psi(x), \quad (2.5)$$

where $M_0(x)$ is the usual bare mass m_0 , modified only by extra contributions at the boundaries

$$M_0(x) = m_0 + (\tilde{c}_t(g_0) - 1) [\delta_{x_0, 1} + \delta_{x_0, L-1}]. \quad (2.6)$$

The lattice Wilson Dirac operator D is given by

$$D = \frac{1}{2} \sum_{\mu} \{ \gamma_{\mu} (\nabla_{\mu}^* + \nabla_{\mu}) - \nabla_{\mu}^* \nabla_{\mu} \}. \quad (2.7)$$

Hermitian γ -matrices are used (we adopt the conventions of ref. [17]). $\nabla_{\mu}, \nabla_{\mu}^*$ are the forward and backward lattice covariant derivatives

$$\nabla_{\mu} \psi(x) = \lambda_{\mu} U(x, \mu) \psi(x + \hat{\mu}) - \psi(x), \quad (2.8)$$

$$\nabla_{\mu}^* \psi(x) = \psi(x) - \lambda_{\mu}^* U(x - \hat{\mu}, \mu)^{\dagger} \psi(x - \hat{\mu}). \quad (2.9)$$

Note that to be able to write the action (2.5) in a more elegant form, we have defined $\psi(x) = 0 = \bar{\psi}(x)$ for $x_0 = 0, L$. The additional $U(1)$ field in (2.8,2.9)

$$\lambda_\mu = \begin{cases} 1 & \text{if } \mu = 0, \\ e^{i\theta/L} & \text{if } \mu > 0, \end{cases} \quad (2.10)$$

corresponds to a free phase in the spatial boundary conditions of the fermions.

Finally S_{SW} is the Sheikholeslami-Wohlert [15] term

$$S_{\text{SW}}[U, \bar{\psi}, \psi] = \frac{i}{4} c_{\text{sw}}(g_0) \sum_{x, \mu, \nu} \bar{\psi}(x) \sigma_{\mu\nu} \mathcal{F}_{\mu\nu}(x) \psi(x), \quad (2.11)$$

where we refer to ref. [17] for the definition of the field $\mathcal{F}_{\mu\nu}$ appearing here. The function $c_{\text{sw}}(g_0)$ is assumed to have a perturbative expansion of the form

$$c_{\text{sw}}(g_0) = c_{\text{sw}}^{(0)} + c_{\text{sw}}^{(1)} g_0^2 + \dots \quad (2.12)$$

Appropriate specification of $c_{\text{sw}}(g_0)$ allows the elimination of all $O(a)$ effects in on shell quantities; the values of the coefficients required for this improvement will be denoted by $c_{\text{sw}}^{(i)*}$. At tree level $c_{\text{sw}}^{(0)*} = 1$ (or $= r$ with general Wilson parameter). The value of the 1-loop coefficient $c_{\text{sw}}^{(1)*}$ is known (see Table 1) and it is independent of N_f ; we note also that c_{sw}^* has been computed non-perturbatively for a range of bare coupling g_0 in the quenched theory [18], [19] and in the unquenched theory with $N_f = 2$ [20].

To define renormalized quark masses from the bare mass m_0 for Wilson fermions requires both additive and multiplicative renormalization:

$$m_{\text{R}} = Z_{\text{m}}(m_0 - m_{\text{c}}). \quad (2.13)$$

where the critical mass m_{c} has a perturbative expansion:

$$m_{\text{c}} = m_{\text{c}}^{(1)} g_0^2 + m_{\text{c}}^{(2)} g_0^4 + \dots \quad (2.14)$$

The coefficients $m_{\text{c}}^{(i)}$ depend on c_{sw} ; in particular the 1-loop coefficient $m_{\text{c}}^{(1)}$, which appears in our computation, depends on the tree value $c_{\text{sw}}^{(0)}$ (see Table 1), but is independent of N_f .

It remains to specify the boundary conditions. Firstly the spatial links $U(x, k)$, $k = 1, 2, 3$, are frozen to fixed $SU(3)$ -elements for the layers at time coordinate $x_0 = 0, L$,

$$U(x, k)|_{x_0=0} = \exp(iaC) = \exp\left[\frac{ia}{L} \text{diag}(\phi_1, \phi_2, \phi_3)\right], \quad (2.15)$$

$$U(x, k)|_{x_0=L} = \exp(iaC') = \exp\left[\frac{ia}{L} \text{diag}(\phi'_1, \phi'_2, \phi'_3)\right]. \quad (2.16)$$

coefficient	value	references
$m_c^{(1)} _{c_{\text{sw}}^{(0)}=0}$	$-0.4342856(3)$	[21],[22],[23]
$m_c^{(1)} _{c_{\text{sw}}^{(0)}=1}$	$-0.2700753495(2)$	[24],[25]
$c_{\text{sw}}^{(1)*}$	$0.26590(7)$	[24],[25]

Table 1: Perturbative coefficients for gauge group SU(3)

Here a is the lattice spacing, and ϕ_i, ϕ'_i are certain [8] dimensionless numbers that depend on one free parameter η . The SF-coupling \bar{g} is defined from the response in the free energy Γ (2.1), to infinitesimal changes in the surface fields by varying η ,

$$\bar{g}^2 = k/\Gamma' , \quad (2.17)$$

where Γ' is the derivative with respect to η at $\eta = 0$, and k is a constant which is fixed by normalizing the leading term in the perturbative expansion

$$\bar{g}^2(L) = g_0^2 + p_1(I)g_0^4 + p_2(I)g_0^6 + \dots \quad (2.18)$$

where here and in the following we often denote the number of lattice points (in a given direction) L/a by I .

The coefficients $c_i(s)$ in the continuum relation (1.1) depend not only on the number of quark flavors N_f but also on the particular choice for the boundary phases ϕ, ϕ' occurring in (2.15,2.16) and on the parameter θ (2.10). Both our perturbative calculation here and simulations reported in [8] and more recently in [6, 4, 5] are restricted to the choice ‘‘A’’ of [8] for the background field and $\theta = \pi/5$.

The coefficients p_i appearing in (2.18) depend on the number of flavors,

$$p_1 = p_{10} + p_{11}N_f , \quad (2.19)$$

$$p_2 = p_{20} + p_{21}N_f + p_{22}N_f^2 . \quad (2.20)$$

The one- and two-loop coefficients p_{10}, p_{20} for the quenched case have been computed in refs. [8], [14] respectively (and for the case of SU(2) in [26]); we note that in these papers the coefficients p_{i0} were denoted by m_i . The one-loop coefficient p_{11} was computed in ref. [17]. Our objective here is to compute the remaining two-loop coefficients p_{21}, p_{22} .

The Callan-Symanzik equation

$$L \frac{\partial}{\partial L} \bar{g}(L) = -\beta(\bar{g}) = b_0 \bar{g}^3 + b_1 \bar{g}^5 + b_2 \bar{g}^7 + \dots \quad (2.21)$$

(the universal 1- and 2-loop beta-function coefficients are given in Appendix A) requires for all values of the improvement coefficients that

$$p_1 = 2b_0 \ln(I) + \bar{p}_1 + \mathcal{O}(1/I), \quad (2.22)$$

$$p_2 - p_1^2 = 2b_1 \ln(I) + \bar{p}_2 + \mathcal{O}(1/I). \quad (2.23)$$

where \bar{p}_i are independent of L/a but dependent on N_f and on c_{sw} . The known values including our results¹ here are summarized in Table 2, where components \bar{p}_{ij} are defined in analogy to (2.19), (2.20).

(i, j)	$\bar{p}_{ij} _{c_{\text{sw}}^{(0)}=0}$	$\bar{p}_{ij} _{c_{\text{sw}}^{(0)}=1}$	references
(1, 0)	0.36828215(13)	0.36828215(13)	[8]
(1, 1)	-0.009868186(4)	-0.034664940(4)	[17]
(2, 0)	0.048091(2)	0.048091(2)	[14]
(2, 1)	-0.00349(3)	0.00978(2) - 0.054641(1) $c_{\text{sw}}^{(1)}$	
(2, 2)	0.000211(3)	0.000209(1)	

Table 2: SF coupling coefficients for gauge group SU(3), background field A and $\theta = \pi/5$

The boundary weight c_t is assumed to have a perturbative expansion of the form

$$c_t(g_0) = 1 + c_t^{(1)} g_0^2 + c_t^{(2)} g_0^4 + \dots \quad (2.24)$$

and similarly for \tilde{c}_t . The freedom of adjusting the boundary weights c_t and \tilde{c}_t to specific functions c_t^* and \tilde{c}_t^* is required for improvement of $\mathcal{O}(a)$ lattice artifacts that are otherwise introduced by the surfaces. The one-loop coefficient $\tilde{c}_t^{(1)*}$ required for improvement of SF correlation functions has been computed in ref. [25] and is independent of N_f . With this knowledge, the perturbative coefficients of c_t^* can be computed to 2-loops from evaluating

¹Reanalysis of the 2-loop $N_f = 0$ data with the method of appendix D has led to errors smaller than the very conservative estimate of [14].

the $O(a)$ lattice artifacts of the SF coupling and demanding deviations from leading continuum behavior to be of $O(a^2)$,

$$\left[p_1 \right]_{c=c^*} = 2b_0 \ln(I) + \bar{p}_1 + O(1/I^2), \quad (2.25)$$

$$\left[p_2 - p_1^2 \right]_{c=c^*} = 2b_1 \ln(I) + \bar{p}_2 + O(1/I^2). \quad (2.26)$$

The coefficients $c_t^{(i)*}$ do depend on the number of fermions,

$$c_t^{(1)*} = c_t^{(1,0)*} + c_t^{(1,1)*} N_f, \quad (2.27)$$

$$c_t^{(2)*} = c_t^{(2,0)*} + c_t^{(2,1)*} N_f + c_t^{(2,2)*} N_f^2. \quad (2.28)$$

The values² of these coefficients are given in Table 3.

coefficient	value	references
$\tilde{c}_t^{(1)*}$	-0.01795(2)	[25],[27]
$c_t^{(1,0)*}$	-0.08900(5)	[7]
$c_t^{(1,1)*}$	0.0191410(1)	[17]
$c_t^{(2,0)*}$	-0.0294(3)	[14]
$c_t^{(2,1)*}$	0.002(1)	
$c_t^{(2,2)*}$	0.0000(1)	

Table 3: SF boundary $O(a)$ improvement coefficients for gauge group $SU(3)$

3 Perturbation expansion to two loops

The perturbative expansion in the bare coupling amounts to an expansion of the gauge field around the induced background field. This has been described in detail in previous publications [7], [26], [14]. In particular we use the gauge fixing procedure as in ref. [7]. In the presence of the abelian background field, both the gluon and quark propagators cannot be computed analytically. The numerical computation of the gluon propagator is described in Section 2 of

²See previous footnote.

ref. [14], and here in Appendix B we give some technical details on how we numerically computed the fermion propagator \mathcal{S} .

An enumeration of the Feynman diagrams contributing to the Schrödinger functional to two-loop order reveals that the coefficients p_{ij} depend on the improvement coefficients and critical mass in the following way:

$$p_{10} = p_1^a + c_t^{(1,0)} p_1^b, \quad (3.1)$$

$$p_{11} = p_1^c + c_t^{(1,1)} p_1^b, \quad (3.2)$$

$$p_{20} - p_{10}^2 = p_2^a + c_t^{(1,0)} p_2^b + [c_t^{(1,0)}]^2 p_2^c + c_t^{(2,0)} p_2^d, \quad (3.3)$$

$$\begin{aligned} p_{21} - 2p_{10}p_{11} = & p_2^e + c_t^{(1,1)} p_2^b + 2c_t^{(1,0)} c_t^{(1,1)} p_2^c + c_t^{(2,1)} p_2^d \\ & + c_t^{(1,0)} p_2^f + \tilde{c}_t^{(1)} p_2^g + c_{\text{sw}}^{(1)} p_2^h + m_c^{(1)} p_2^i, \end{aligned} \quad (3.4)$$

$$p_{22} - p_{11}^2 = p_2^j + [c_t^{(1,1)}]^2 p_2^c + c_t^{(2,2)} p_2^d + c_t^{(1,1)} p_2^f. \quad (3.5)$$

All the coefficients coming from diagrams not involving the quarks have been computed in [14]. Here we recall that only two of the coefficients can be given in closed form:

$$p_1^b = p_2^d = -\frac{2}{I}, \quad (3.6)$$

$$p_2^c = \frac{2}{I} - \frac{4}{I^2} + \mathcal{O}(1/I^5), \quad (3.7)$$

whereas the others require careful numerical evaluation. The contributions p_1^a , p_2^a and p_2^b are tabulated in Table 1 of ref. [14].

As for the diagrams involving the quarks, the one-loop coefficient

$$p_1^c = -\frac{1}{k} \Gamma_1^{c'}, \quad (3.8)$$

with

$$\Gamma_1^{c'} = -\text{tr} \mathcal{S} \frac{\partial \mathcal{S}^{-1}}{\partial \eta} \Big|_{\eta=0}, \quad (3.9)$$

has been computed in ref.[17].

It remains to compute the coefficients $p_2^e, p_2^f, p_2^g, p_2^h, p_2^i, p_2^j$. The contributions p_2^g, p_2^h, p_2^i are very simple because they are obtained by differentiating the one-loop contribution p_1^c with respect to the bare parameters e.g.

$$\Gamma_2^{h'} = \text{tr} \left[\mathcal{S} \frac{\partial \mathcal{S}^{-1}}{\partial \eta} \mathcal{S} \frac{\partial \mathcal{S}^{-1}}{\partial c_{\text{sw}}(0)} - \mathcal{S} \frac{\partial^2 \mathcal{S}^{-1}}{\partial \eta \partial c_{\text{sw}}(0)} \right] \Big|_{\eta=0}, \quad (3.10)$$

and similarly for p_2^g, p_2^i . The contributions are diagrammatically represented in Fig. 1a where the filled circle indicates the insertion obtained by differentiation with respect to one of the bare parameters (the differentiation with respect to η is not indicated).

The contribution p_2^f arises from the correlation of a boundary term in the pure gluon part of the action with the quark-antiquark 1-gluon vertex given in diagram Fig. 1b.

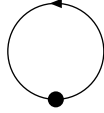


Fig. 1a

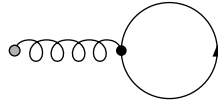


Fig. 1b

The remaining part p_2^e of p_{21} comes from the four diagrams in Fig. 2. The fermion big-mac diagram Fig. 2c is the technically most difficult diagram; the rest of the diagrams are simpler because they are essentially products of 1-loop diagrams.

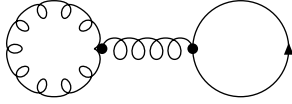


Fig. 2a

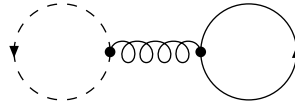


Fig. 2b

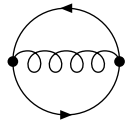


Fig. 2c

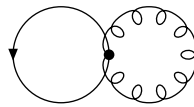


Fig. 2d

Finally there is only one as yet unmentioned contribution p_2^j to p_{22} , which is basically the product of two fermion tadpoles depicted in Fig. 3.

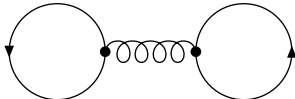


Fig. 3

Despite optimization of the code in various respects by e.g. making use of all symmetry properties, the CPU-time for the computation which is dominated by the big-mac diagram in Fig. 2c, is rather costly growing rapidly as $(L/a)^5$. All diagrams were computed using double precision arithmetic to at least $L/a = 32$, for two cases $c_{\text{sw}}^{(0)} = 1$ and $c_{\text{sw}}^{(0)} = 0$. The numerical results for $p_2^e, p_2^f, p_2^g, p_2^h, p_2^i, p_2^j$ for $c_{\text{sw}}^{(0)} = 1$, and for p_2^e, p_2^i, p_2^j for $c_{\text{sw}}^{(0)} = 0$, are given in Appendix C in Tables 4,5 and 6 respectively.

We have various stringent tests (as in [26]) to check our numbers; firstly the full code using sums in position space was compared on the smallest lattices with a slow but independent code (many of whose subroutines had been well tested in previous computations) making sums in momentum space. Secondly gauge parameter independence of the p_2^x was checked. Thirdly it was checked that the full code reproduced numbers for partial sums satisfying all analytically known symmetries, before these were actually used to reduce the number of terms in order to speed up the program execution time. Finally the fact that the I -dependence for p_{21}, p_{22} (depending on the value of $c_{\text{sw}}^{(0)}$ as described in the next section) was as expected from general considerations, gave a further consistency check.

4 Analysis of the a/L dependence

The generically expected behavior for 2-loop lattice Feynman diagrams suggests an asymptotic expansion for the two-loop coefficients p_2^x of the form (recall $I = L/a$)

$$p_2^x = \sum_{n=n^x}^{\infty} [r_n^x + s_n^x \ln(I) + t_n^x \ln^2(I)] I^{-n}. \quad (4.1)$$

The coefficients of these expansions are extracted from the series of finite lattices (see Appendix C). The method we used here to extract these numbers

together with an estimate of their systematic errors is described in some detail in Appendix D.

4.1 The case $c_{\text{sw}}^{(0)} = 1$

4.1.1 The continuum behavior of p_{22}

Let us start with the simpler case of p_{22} where the non-trivial contributions come from only p_2^f and p_2^j . For p_2^f we have $n^f = 1$ and $t_n^f = 0$ for all n . Our result is:

$$s_1^f = -0.03375(4), \quad (4.2)$$

$$r_1^f = -0.0734(4). \quad (4.3)$$

The contribution p_2^j on the other hand has a finite non-trivial continuum limit $n^j = 0$, $s_0^j = 0$. As for the coefficients t_n^j these are generally non-zero, since the diagram is a product of one-loop diagrams, but $t_0^j = t_1^j = 0$. For the leading coefficients we find

$$r_0^j = 0.000210(3), \quad (4.4)$$

$$s_1^j = 0.0003(14), \quad (4.5)$$

$$r_1^j = 0.003(9). \quad (4.6)$$

The extracted value of s_1^j above is unfortunately not very precise but consistent with the value 0.000646 obtained from the equation

$$s_1^j + c_t^{(1,1)*} s_1^f = 0 \quad (4.7)$$

that we expect from $O(a)$ improvement.

If we now analyze the series for $p_2^j + c_t^{(1,1)*} p_2^f$ with the known value for $c_t^{(1,1)*}$ with the assumption that the equation (4.7) is fulfilled i.e.

$$p_2^j + c_t^{(1,1)*} p_2^f = r_0^{fj} + \frac{r_1^{fj}}{I} + \frac{r_2^{fj} + s_2^{fj} \ln(I) + t_2^{fj} \ln^2(I)}{I^2} + \dots \quad (4.8)$$

we get

$$r_0^{fj} = 0.000209(1), \quad (4.9)$$

$$r_1^{fj} = -0.0008(2). \quad (4.10)$$

Thus we obtain a refined estimate of $\bar{p}_{22} = r_0^{fj}$ recorded in Table 2. Finally we estimate the improvement coefficient $c_t^{(2,2)*}$ through

$$c_t^{(2,2)*} = \frac{1}{2} r_1^{fj} + \left(c_t^{(1,1)*} \right)^2 = 0.0000(1). \quad (4.11)$$

4.1.2 The continuum behavior of p_{21}

First of all, the expansion of p_2^g has the same structure as that of p_2^f i.e. it has a trivial continuum limit $n^g = 1$ and also the coefficients $t_n^g = 0$ for all n . The analysis yields

$$s_1^g = 0.0338(3), \quad (4.12)$$

$$r_1^g = 0.115(2). \quad (4.13)$$

p_2^h on the other hand has a non-trivial finite continuum limit $n^h = 0$, $s_0^h = 0$ and $t_n^h = 0$ for all n . Our results for the leading terms are

$$r_0^h = -0.054641(1), \quad (4.14)$$

$$s_1^h = -0.0252(2), \quad (4.15)$$

$$r_1^h = 0.032(1). \quad (4.16)$$

The mass insertion term p_2^i has a linear divergence, $n^i = -1$ but $s_{-1}^i = s_0^i = 0$ and $t_n^i = 0$ for all n . For the leading terms we find

$$r_{-1}^i = 0.009568(1), \quad (4.17)$$

$$r_0^i = 0.01198(11). \quad (4.18)$$

Finally the contribution p_2^e has an expansion of the form

$$p_1^e = r_{-1}^e I + r_0^e + s_0^e \ln(I) + \frac{r_1^e + s_1^e \ln(I)}{I} + \dots \quad (4.19)$$

t_1^e is expected to be zero because of tree level improvement and the data is consistent with this expectation. For this coefficient our analysis gives

$$r_{-1}^e = 0.002586(2), \quad (4.20)$$

$$s_0^e = -0.0012(3), \quad (4.21)$$

$$r_0^e = 0.0141(16). \quad (4.22)$$

On the other hand we know that the linear divergences must cancel and hence

$$r_{-1}^e = -m_c^{(1)} r_{-1}^i, \quad (4.23)$$

should hold. Indeed from (4.23) we find the value 0.0025841(3) which serves as an additional consistency check. In the next step we thus assume the cancellation of linear divergences and analyze

$$p_2^e + m_c^{(1)} p_2^i = r_0^{ei} + s_0^{ei} \ln(I) + \frac{r_1^{ei} + s_1^{ei} \ln(I) + t_1^{ei} \ln^2(I)}{I} + \dots \quad (4.24)$$

From this series we could get the still somewhat rough estimates of the continuum behavior

$$s_0^{ei} = -0.00104(12), \quad (4.25)$$

$$r_0^{ei} = 0.0099(7). \quad (4.26)$$

The Callan-Symanzik equation (2.21) (which incidentally requires $t_0 = 0$) requires the logarithmic divergence s_0^{ei} to coincide with $2b_{11} = -0.0010159$, and our estimate (4.25) agrees with this within errors. We are thus justified to assume this to actually be the case and continue to analyze

$$p_2^e + m_c^{(1)} p_2^i - 2b_{11} \ln(I) = r_0^{ei} + \frac{r_1^{ei} + s_1^{ei} \ln(I) + t_1^{ei} \ln^2(I)}{I} + \dots \quad (4.27)$$

to obtain an improved estimate for the coefficient

$$r_0^{ei} = 0.00978(2). \quad (4.28)$$

The value for the coefficient \bar{p}_{21} in Table 2 comes from

$$\bar{p}_{21} = r_0^{ei} + c_{sw}^{(1)*} r_0^h. \quad (4.29)$$

We also obtain (unfortunately rather poor) estimates for the $O(a)$ coefficients

$$s_1^{ei} = -0.0016(17), \quad (4.30)$$

$$r_1^{ei} = -0.003(7). \quad (4.31)$$

In fact improvement requires

$$-s_1^{ei} = c_t^{(1,1)*} s_1^b + c_t^{(1,0)*} s_1^f + \tilde{c}_t^{(1)*} s_1^g + c_{sw}^{(1)*} s_1^h. \quad (4.32)$$

Using the previously obtained [13] values $r_1^b = 0.16831(84)$ and $s_1^b = 0.27848(40)$ gives $s_1^{ei} = -0.00103(7)$ which is consistent with but much more accurate than our estimate above.

Finally the most accurate value we could obtain for improvement coefficient $c_t^{(2,1)*}$ was extracted by forming the combination

$$p_2^e + m_c^{(1)} p_2^i - 2b_{11} \ln(I) + c_t^{(1,1)*} p_2^b + c_t^{(1,0)*} p_2^f + \tilde{c}_t^{(1)*} p_2^g + c_{sw}^{(1)*} p_2^h, \quad (4.33)$$

and analyzing the series with the assumption it has the form

$$r_0^x + \frac{r_1^x}{I} + \frac{r_2^x + s_2^x \ln(I) + t_2^x \ln^2(I)}{I^2} + \dots \quad (4.34)$$

thereby obtaining the estimate

$$r_1^x = 0.011(2), \quad (4.35)$$

and finally

$$c_t^{(2,1)*} = 2c_t^{(1,0)*} c_t^{(1,1)*} + \frac{1}{2} r_1^x = 0.002(1). \quad (4.36)$$

4.2 The case $c_{\text{sw}}^{(0)} = 0$

The analysis of the data for the case $c_{\text{sw}}^{(0)} = 0$ is completely analogous to that for $c_{\text{sw}}^{(0)} = 1$ above, except for the fact that we can simply ignore also all other improvement coefficients. Thus e.g. for p_{22} only p_2^j has to be analyzed, and with the same ansatz as before we find

$$r_0^j = 0.000211(3). \quad (4.37)$$

For p_{21} we only take into account p_2^e and p_2^i . Again we find that the linear divergences cancel (with the appropriate value of $m_c^{(1)}$) and the coefficient of $\ln(I)$ reproduces $2b_{11}$ within errors. Finally we fit

$$p_2^e + m_c^{(1)} p_2^i - 2b_{11} \ln(I) = r_0^x + \frac{r_1^x + s_1^x \ln(I) + t_1^x \ln^2(I)}{I} + \dots, \quad (4.38)$$

and the ensuing estimate of r_0^x gives us the value of \bar{p}_{21} quoted in Table 2 for this case.

5 Applications

5.1 The relation of $\alpha_{\overline{\text{MS}}}$ to α_{SF}

To obtain the coefficients $c_i(s)$ in eq.(1.1) from our computation above, we have to use the known results for the coefficients appearing in the relation between $\alpha_{\overline{\text{MS}}}$ and α_0 :

$$\alpha_{\overline{\text{MS}}}(s/a) = \alpha_0 + d_1(s)\alpha_0^2 + d_2(s)\alpha_0^3 + \dots \quad (5.1)$$

with

$$d_1(s) = \sum_{r=0}^1 N_f^r \left\{ -8\pi b_{0r} \ln(s) + d_{1r} \right\}, \quad (5.2)$$

$$d_2(s) = d_1(s)^2 + \sum_{r=0}^1 N_f^r \left\{ -32\pi^2 b_{1r} \ln(s) + d_{2r} \right\}. \quad (5.3)$$

The coefficients d_{ir} (and the β -function coefficients) are given in Appendix A.

The coefficients $c_i(s)$ in eq.(1.1) are now obtained through

$$c_1(s) = -8\pi b_0 \ln(s) + \sum_{r=0}^1 N_f^r \{d_{1r} - 4\pi \bar{p}_{1r}\}, \quad (5.4)$$

$$c_2(s) = c_1(s)^2 - 32\pi^2 b_1 \ln(s) + \sum_{r=0}^2 N_f^r \{d_{2r} - 16\pi^2 \bar{p}_{2r}\}. \quad (5.5)$$

Now it is clear that since eq.(1.1) is a relation between continuum quantities all coefficients c_r must be independent of the lattice bare parameters, which serves as a further consistency check on the computations. This has already been observed at the 1-loop level i.e. from Table 2 and eqns.(A.2,A.8) one sees that $d_{11} - 4\pi \bar{p}_{11}$ is independent of $c_{\text{sw}}^{(0)}$. At the two loop level, since $d_{22} = 0$ (there is no term $\propto N_f^2$ in (5.3)), we should find that \bar{p}_{22} is independent of c_{sw} . Indeed our numerical results in Table 2 are consistent with this expectation. Finally $d_{21} - 16\pi^2 \bar{p}_{21}$ should be independent of c_{sw} ; unfortunately this cannot be checked at present because the computation of the d_{21} for $c_{\text{sw}} \neq 0$ is not yet complete [28]. However demanding the equality would require

$$d_{21}|_{N=3, c_{\text{sw}}^{(0)}=1} = 1.685(9) - 8.6286(2)c_{\text{sw}}^{(1)}, \quad (5.6)$$

which will serve as a good consistency check for the (general $\text{SU}(N)$) computation above in progress [28]. In fact the coefficient of $c_{\text{sw}}^{(1)}$ above, $16\pi^2 r_0^h$, is already independently checked because r_0^h should be related to the coefficient K_1 in (A.8) through

$$r_0^h = \frac{1}{4\pi} \left. \frac{dK_1(x)}{dx} \right|_{x=1}, \quad (5.7)$$

and this is fulfilled numerically to good precision.

Putting all our numerical results together we find for $N = 3$

$$c_1(s) = -8\pi b_0 \ln(s) + 1.255621(2) + 0.0398629(2)N_f, \quad (5.8)$$

$$c_2(s) = c_1(s)^2 - 32\pi^2 b_1 \ln(s) + 1.197(10) + 0.140(6)N_f - 0.0330(2)N_f^2. \quad (5.9)$$

This two-loop connection between the two different couplings determines the difference between the non-universal three-loop coefficients of their respective

β -functions:

$$b_2 = b_2^{\overline{\text{MS}}} + \frac{b_1 c_1(1)}{4\pi} - \frac{b_0 [c_2(1) - c_1(1)^2]}{16\pi^2}. \quad (5.10)$$

Since the three-loop β -function in the $\overline{\text{MS}}$ -scheme is known we can obtain the SF 3-loop beta function coefficient for the background field A (and $\theta = \pi/5$) e.g. :

$$b_2|_{N_f=0} = 0.482(7) \times (4\pi)^{-3}, \quad (5.11)$$

$$b_2|_{N_f=2} = 0.064(10) \times (4\pi)^{-3}. \quad (5.12)$$

The perturbative coefficients will find their application when the SF-coupling has been measured over a wide range of energies. Once the SF-coupling \bar{g} is known for small box size, it is to be converted to the $\overline{\text{MS}}$ -coupling at high energy. One could conventionally choose the mass of the neutral weak boson M_Z as a scale here. Another procedure — attractive for asymptotically free theories — is to extract the Λ -parameter which is simply related to the behavior at asymptotically large energy. It is a renormalization group invariant given by

$$\Lambda_{\text{SF}} = L^{-1} (b_0 \bar{g}^2)^{-b_1/(2b_0^2)} e^{-1/(2b_0 \bar{g}^2)} \exp \left\{ - \int_0^{\bar{g}} dg \left[\frac{1}{\beta(g)} + \frac{1}{b_0 g^3} - \frac{b_1}{b_0^2 g} \right] \right\}. \quad (5.13)$$

The conversion to $\Lambda_{\overline{\text{MS}}}$ then amounts to an additional known factor:

$$\Lambda_{\overline{\text{MS}}} = \Lambda_{\text{SF}} \exp \left(\frac{c_1(1)}{8\pi b_0} \right) \quad (5.14)$$

$$= 2.382035(3) \Lambda_{\text{SF}}, \quad \text{for } N_f = 2. \quad (5.15)$$

If we insert a small $\bar{g}(L)$ belonging to a very small L (in physical units) into formula (5.13), then the exponentiated integral is close to unity. Knowledge of the three loop term will give some estimate of the systematic error which will definitely be less than the statistical error in the near future.

5.2 The step scaling function

A central quantity in the ALPHA collaboration's approach is the step scaling function which generalizes the β -function to finite rescalings,

$$\sigma(s, u) = \bar{g}^2(sL)|_{\bar{g}^2(L)=u}. \quad (5.16)$$

We remind the reader that we use a mass independent renormalization scheme and set the quark mass to zero. On the lattice, σ emerges as the continuum limit of a finite lattice spacing approximant Σ ,

$$\sigma(s, u) = \lim_{a \rightarrow 0} \Sigma(s, u, a/L). \quad (5.17)$$

Due to the absence of chiral symmetry before the continuum limit is taken one has to precisely specify a zero mass condition with the cutoff in place. In the numerical simulations a certain unambiguous definition based on the PCAC relation is adopted. This leads to $I = L/a$ dependent expansion coefficients $m_c^{(i)}(I)$, which only as $I \rightarrow \infty$ go over to the convention independent values $m_c^{(0)} = 0$ and $m_c^{(1)}$ in Table 1. Only the latter are presently known to us. For the extrapolations in the previous section (including $O(a)$ improvement) this is of no concern. The following perturbative estimation of the full (all orders in a) lattice artifacts would however be more realistic with finite I mass expansion coefficients and is hence only given to get a first idea here. An improved version will be published elsewhere.

All perturbative information about the convergence speed of Σ for $s = 2$ is conveniently summarized in coefficients $\delta_{nj}(a/L)$ defined by

$$\delta(u, a/L) = \frac{\Sigma(2, u, a/L) - \sigma(2, u)}{\sigma(2, u)} \quad (5.18)$$

$$= \sum_{n=1} u^n \sum_{j=0}^n N_{\text{f}}^j \delta_{nj}(a/L). \quad (5.19)$$

Setting $\Delta p_{ij}(I) = p_{ij}(2I) - p_{ij}(I)$ we have

$$\delta_{10} = \Delta p_{10} - 2b_{00} \ln(2), \quad (5.20)$$

$$\delta_{11} = \Delta p_{11} - 2b_{01} \ln(2), \quad (5.21)$$

$$\delta_{20} = \Delta p_{20} - 2b_{10} \ln(2) - 2\Delta p_{10}(p_{10} + b_{00} \ln(2)), \quad (5.22)$$

$$\delta_{21} = \Delta p_{21} - 2b_{11} \ln(2) - 2\Delta p_{11}(p_{10} + b_{00} \ln(2)) - 2\Delta p_{10}(p_{11} + b_{01} \ln(2)), \quad (5.23)$$

$$\delta_{22} = \Delta p_{22} - 2\Delta p_{11}(p_{11} + b_{01} \ln(2)). \quad (5.24)$$

All the δ_{nj} decay with an asymptotic rate proportional to $(a/L)^2$ in the $O(a)$ improved theory. We are free to use δ to cancel perturbative finite a effects from Monte Carlo data, as pointed out in [34]. For this purpose one

uses the same improvement coefficients as in the simulation and the expansion of m_c for finite lattice spacing. Only for cases where nonperturbative improvement coefficients are used in the simulation, like c_{sw} , one replaces these by the leading perturbative expressions. Fig.1 gives an impression of

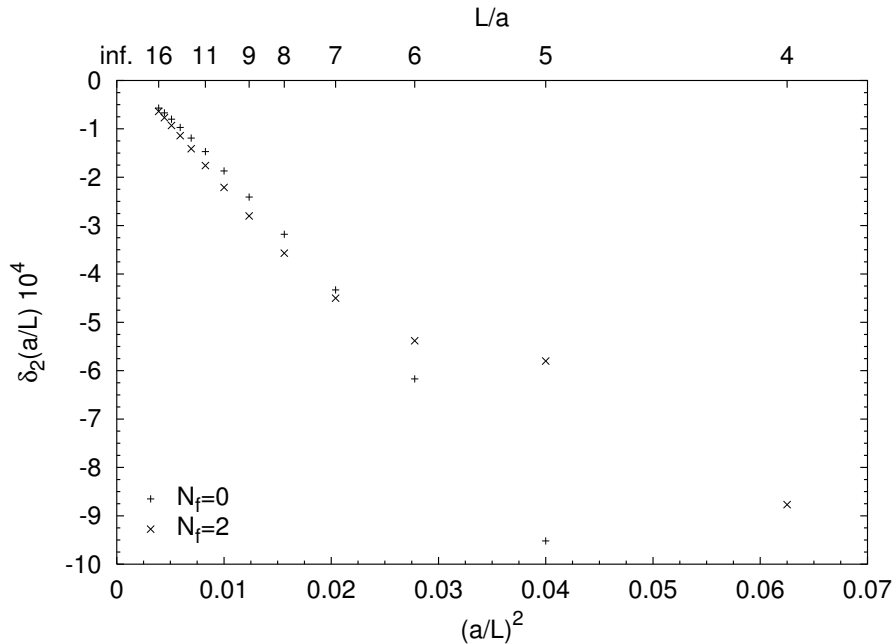


Figure 1: Two loop contribution to lattice artifacts.

the two loop artifacts for zero and two flavours. They are reasonably small and show the expected decay pattern.

Acknowledgements

We would like to thank Juri Rolf, Stefan Sint and Rainer Sommer for useful discussions and correspondence.

A. The 2-loop relation between $\alpha_{\overline{\text{MS}}}$ and α_0

The coefficients d_{ir} appearing in the the relation between $\alpha_{\overline{\text{MS}}}$ and α_0 Eqs.(5.2), (5.3) have the form for general gauge group $\text{SU}(N)$

$$d_{10} = -\frac{\pi}{2N} + k_1 N, \quad (\text{A.1})$$

$$d_{11} = K_1, \quad (\text{A.2})$$

$$d_{20} = \frac{3\pi^2}{8N^2} + k_2 + k_3 N^2, \quad (\text{A.3})$$

$$d_{21} = \frac{K_2}{N} + K_3 N. \quad (\text{A.4})$$

The coefficients k_i which have been computed in [9] and checked by the authors of ref. [10] are given by

$$k_1 = 2.135730074078457(2), \quad (\text{A.5})$$

$$k_2 = -2.8626215972(6), \quad (\text{A.6})$$

$$k_3 = 1.24911585(3). \quad (\text{A.7})$$

The coefficient K_1 is a function of $c_{\text{sw}}^{(0)}$ and Wilson's parameter r . In our computations we always set $r = 1$ and hence only indicate the dependence on $c_{\text{sw}}^{(0)}$ i.e. $K_1 = K_1(c_{\text{sw}}^{(0)})$. We have ³

$$K_1(x) = -0.08414443(8) + 0.063419(1)x - 0.375024(1)x^2. \quad (\text{A.8})$$

Similarly we have $K_r = K_r(c_{\text{sw}}^{(0)}, c_{\text{sw}}^{(1)})$ for $r = 2, 3$. So far only the pure Wilson case has been computed in ref. [11]

$$K_2(0, 0) = 0.1890(2), \quad (\text{A.9})$$

$$K_3(0, 0) = -0.1579(3). \quad (\text{A.10})$$

The extension of the computation to the case $c_{\text{sw}} \neq 0$ is now under way [28].

The universal coefficients of the beta-function are given by

$$b_i = b_{i0} + b_{i1} N_f, \quad i = 0, 1, \quad (\text{A.11})$$

with

$$b_{00} = \frac{1}{(4\pi)^2} \frac{11N}{3}, \quad (\text{A.12})$$

$$b_{01} = -\frac{1}{(4\pi)^2} \frac{2}{3}, \quad (\text{A.13})$$

³To give a standard reference to the computation of K_1 is difficult. The precise result in (A.8) comes from Stefan Sint [29]. The result in eq.(29) of the recent paper [30] agrees with this. The computation of $K_1(0)$ was first presented in refs. [31], [32] and a more precise value is given in [11]. The extension of the calculation to $c_{\text{sw}} \neq 0$ was first presented in [33], however there are some errors in the result quoted there (of which the authors were conscious but unfortunately they did not publish an erratum).

$$b_{10} = \frac{1}{(4\pi)^4} \frac{34N^2}{3}, \quad (\text{A.14})$$

$$b_{11} = -\frac{1}{(4\pi)^4} \left(\frac{13N}{3} - \frac{1}{N} \right), \quad (\text{A.15})$$

and the 3-loop beta function coefficient in the MS-scheme [35] is given by

$$b_2^{\overline{\text{MS}}} = b_{20}^{\overline{\text{MS}}} + b_{21}^{\overline{\text{MS}}} N_f + b_{22}^{\overline{\text{MS}}} N_f^2, \quad (\text{A.16})$$

with

$$b_{20}^{\overline{\text{MS}}} = \frac{1}{(4\pi)^6} \frac{2857N^3}{54}, \quad (\text{A.17})$$

$$b_{21}^{\overline{\text{MS}}} = -\frac{1}{(4\pi)^6} \left(\frac{1709N^2}{54} - \frac{187}{36} - \frac{1}{4N^2} \right), \quad (\text{A.18})$$

$$b_{22}^{\overline{\text{MS}}} = \frac{1}{(4\pi)^6} \left(\frac{56N}{27} - \frac{11}{18N} \right). \quad (\text{A.19})$$

B. The free fermion propagator in the abelian background field

The Wilson-Dirac operator D , which is now taken to include the Sheikoleslami-Wohlert term, is diagonal in momentum and color space for the background field under consideration. We hence assume these fixed and discuss the inversion in time and Dirac-spin space. The calculational technique is adapted from the calculation the background field gluon propagator in [26, 14].

The propagator will be entirely constructed from solutions to the homogeneous equations

$$(D\psi^f)(t) = 0 \quad \text{with } P_+\psi^f(0) = \psi_+^f(0) = 0, \quad (\text{B.1})$$

$$(D\psi^b)(t) = 0 \quad \text{with } P_-\psi^b(T) = \psi_-^b(T) = 0 \quad (\text{B.2})$$

with projectors $P_\pm = \frac{1}{2}(1 \pm \gamma_0)$. In each case there are two independent solutions, which are constructed by forward (backward) recurrence in t for ψ_f (ψ_b) starting from the $t = 0$ ($t = T$) boundary. We assemble the two solutions into two columns in ψ_f , ψ_b . Using pseudo hermiticity, $D^\dagger = \gamma_5 D \gamma_5$, the defining equation

$$D\mathcal{S}(t, t') = \delta_{t, t'}, \quad 0 < t, t' < T, \quad (\text{B.3})$$

and the fact that in a matrix sense S must also be the left inverse to D we derive

$$\mathcal{S}(t, t') = \begin{cases} \psi^f(t)V\psi^b(t')^\dagger\gamma_5 & t < t' \\ \psi^b(t)V^\dagger\psi^f(t')^\dagger\gamma_5 & t > t'. \end{cases} \quad (\text{B.4})$$

Here V is a two by two matrix acting on the index that labels independent solutions. Inspection of the propagator equation at $t' = t \pm 1$ yields in addition

$$\mathcal{S}(t, t) = \psi_-^f(t)V\psi_-^b(t)^\dagger\gamma_5 + \psi_+^b(t)V^\dagger\psi_+^f(t)^\dagger\gamma_5 \quad (\text{B.5})$$

and

$$\psi_-^f(t)V\psi_-^b(t)^\dagger\gamma_5 = \psi_-^b(t)V^\dagger\psi_-^f(t)^\dagger\gamma_5, \quad (\text{B.6})$$

$$\psi_+^b(t)V^\dagger\psi_+^f(t)^\dagger\gamma_5 = \psi_+^f(t)V\psi_+^b(t)^\dagger\gamma_5. \quad (\text{B.7})$$

To determine V we exploit (B.3) at $t = t'$,

$$\begin{aligned} 1 &= -\psi_+^f(t-1)V\psi_-^b(t)^\dagger\gamma_5 + \psi_+^b(t-1)V^\dagger\psi_-^f(t)^\dagger\gamma_5 \\ &\quad + \psi_-^f(t+1)V\psi_+^b(t)^\dagger\gamma_5 - \psi_-^b(t+1)V^\dagger\psi_+^f(t)^\dagger\gamma_5. \end{aligned} \quad (\text{B.8})$$

Now V can be isolated with the help of (B.6), (B.7) and

$$\psi^f(t-1)^\dagger\gamma_5\psi_-^f(t) - \psi^f(t)^\dagger\gamma_5\psi_+^f(t-1) = 0, \quad (\text{B.9})$$

whose left hand side is shown to be t -independent by the homogeneous Dirac equation and vanishes for $t = 1$. The final result can be written as

$$(V^\dagger)^{-1} = \psi_-^f(1)^\dagger\gamma_5\psi_+^b(0). \quad (\text{B.10})$$

C. Tables of expansion coefficients

In this appendix we list perturbative finite lattice input data that went into our analysis. Numbers have been truncated such that roundoff errors affect the last digit only.

I	p_2^e	p_2^f	p_2^g
3	0.01406000332624868	-0.0182407224873773	0.02748117066751495
4	0.01838971613803814	-0.0190839262114088	0.02912977487693198
5	0.0213244240582013	-0.0182173759776234	0.0272378718296281
6	0.0240118520229137	-0.0171194898351334	0.0248632085828385
7	0.0266888600910630	-0.016021619058412	0.0226936034816730
8	0.029366920333954	-0.014993754483268	0.0208214421618160
9	0.032033898489622	-0.014058323610653	0.0192191961300145
10	0.034684945753779	-0.013217310231851	0.0178425484742938
11	0.037320642901569	-0.012464162363595	0.0166512309905875
12	0.039943407218950	-0.011789492952359	0.015612173517774
13	0.042555797334290	-0.011183638952885	0.014698916407548
14	0.045159985052289	-0.010637686960534	0.013890391073651
15	0.04775768717127	-0.010143794730699	0.013169772817157
16	0.05035023257788	-0.009695210528629	0.012523543034029
17	0.05293864891550	-0.00928617606722	0.011940757139333
18	0.05552373638933	-0.00891179536156	0.011412482658586
19	0.05810612401759	-0.00856790398265	0.010931369933803
20	0.06068631107488	-0.00825095161082	0.010491323683996
21	0.06326469747537	-0.00795790134914	0.010087250557429
22	0.06584160619894	-0.00768614535208	0.009714863852334
23	0.06841730002735	-0.00743343490502	0.009370531360667
24	0.07099199418417	-0.00719782275317	0.009051155905983
25	0.07356586599137	-0.00697761558627	0.008754080827932
26	0.07613906232516	-0.00677133484944	0.008477014637251
27	0.0787117066394	-0.00657768434489	0.008217970511475
28	0.0812838974813	-0.00639552336330	0.007975217365077
29	0.0838557242252	-0.00622384432090	0.007747240012744
30	0.0864272578552	-0.00606175407446	0.007532706527406
31	0.0889985593460	-0.00590845824714	0.007330441330203
32	0.0915696803402	-0.00576324802706	0.007139402877142

Table 4: List of I -dependent coefficients p_2^e , p_2^f and p_2^g for $c_{\text{sw}}^{(0)} = 1$.

I	p_2^h	p_2^i	p_2^j
3	-0.0472978469844831	0.02748117066751495	0.00036913190875759
4	-0.0522497820522355	0.0406644614491804	-0.00019279262914480
5	-0.0544132909735601	0.0518711757366513	0.000062922280309919
6	-0.0555160735660078	0.0625335624963019	0.00024693874361661
7	-0.0561252173383393	0.0729651117622647	0.00032829652675201
8	-0.0564756935876461	0.0832353491549959	0.00035889080255099
9	-0.0566798625246374	0.0933761748042426	0.00036802392907154
10	-0.0567967356276605	0.103414110425804	0.00036829902719101
11	-0.0568594539035442	0.113371699857364	0.00036493229776592
12	-0.056887606070495	0.123266779814805	0.00036013282273909
13	-0.056893249514880	0.133112866383861	0.00035486899918541
14	-0.056884053136243	0.142920056704081	0.00034957573793481
15	-0.056865026658050	0.152695918495843	0.00034444805110225
16	-0.056839514713774	0.162446191871116	0.00033956882844280
17	-0.056809789874931	0.172175297258459	0.0003349670866427
18	-0.056777417868152	0.181886691902227	0.0003306456480143
19	-0.056743488785825	0.191583119155590	0.0003265947619586
20	-0.056708767026702	0.201266784482244	0.0003227989929269
21	-0.056673790607995	0.210939481638856	0.0003192407628410
22	-0.056638938178912	0.220602684697517	0.0003159021777408
23	-0.056604474988832	0.230257616284550	0.0003127659514888
24	-0.056570584880899	0.239905298968026	0.0003098158454325
25	-0.056537392847533	0.249546594496119	0.0003070368462269
26	-0.056504981113718	0.259182234133082	0.0003044152025451
27	-0.056473400720539	0.268812842375392	0.0003019383874879
28	-0.056442679941137	0.278438955679912	0.0002995950240854
29	-0.056412830441785	0.288061037388928	0.0002973747949003
30	-0.056383851821358	0.297679489724326	0.0002952683474247
31	-0.056355734973936	0.307294663501017	0.0002932672016335
32	-0.056328464590232	0.31690686604973	0.0002913636629602

Table 5: List of I -dependent coefficients p_2^h , p_2^i and p_2^j for $c_{\text{sw}}^{(0)} = 1$.

I	p_2^e	p_2^i	p_2^j
3	0.002930793635704460	0.01113927564510310	-0.00081995809255674
4	0.00648721649586021	0.02176506549404950	-0.00095088311404386
5	0.01042316816041390	0.0326987791899857	-0.00047704024765898
6	0.0147884221405374	0.0441250945952050	-0.00017002734632304
7	0.0194100790766652	0.0557968441900837	-0.000012571985852322
8	0.0241548411409164	0.0675196648718815	0.000069240759237721
9	0.028948291534668	0.0791944332878618	0.00011551757360719
10	0.033752733950337	0.0907802022873036	0.00014436115981723
11	0.038549666950648	0.102264260790802	0.00016392305375706
12	0.043330159467278	0.113646262219098	0.00017808308496443
13	0.048090083743491	0.124930880299287	0.00018883175180516
14	0.05282779555547	0.136124585602541	0.00019727388656343
15	0.05754297570840	0.147234255392045	0.00020407010116580
16	0.06223602393897	0.158266580822338	0.00020964219355829
17	0.06690772585583	0.169227824652203	0.00021427470438615
18	0.07155906252343	0.180123737178240	0.00021816831762828
19	0.07619109889499	0.190959545294390	0.00022146967768869
20	0.08080491792206	0.201739975291261	0.00022428900150278
21	0.08540158202310	0.212469290287585	0.00022671102155128
22	0.08998211127935	0.223151332698423	0.00022880209115049
23	0.09454747195837	0.233789566873300	0.00023061497375955
24	0.0990985714169	0.244387119503159	0.00023219217419543
25	0.1036362569094	0.254946816719166	0.0002335683174515
26	0.1081613167382	0.265471217523167	0.0002347718854825
27	0.1126744827534	0.275962643571370	0.0002358265093730
28	0.1171764335743	0.286423205525826	0.0002367519464219
29	0.1216677981308	0.296854826274766	0.0002375648294884
30	0.1261491592962	0.307259261350171	0.0002382792488587
31	0.1306210574330	0.31763811686605	0.0002389072090909
32	0.1350839937928	0.32799286527967	0.0002394589912651

Table 6: List of I -dependent coefficients p_2^e , p_2^i and p_2^j for $c_{\text{sw}}^{(0)} = 0$.

D. Extrapolation of lattice perturbation theory

In this appendix we discuss a modified method to extract the continuum limit behavior of lattice Feynman diagrams. That is we assume to have precise results $F(I)$ (for a given diagram or a sum of diagrams) for a range of $I = L/a$, $I_1 < I_2 < \dots < I_n$ (typical subsets of I are $2, \dots, 32$), and the goal is to determine the leading and subleading behavior as $I \rightarrow \infty$.

The precision of the data is limited by roundoff effects. We treat the roundoff errors $\delta_F(I)$ as normally distributed superimposed noise, independent for different I . The most optimistic assumption for results from double precision (real*8) arithmetic would be

$$\delta_F(I) = \epsilon |F(I)|, \quad \epsilon \sim 10^{-14}, \quad (\text{D.1})$$

but in general this is an underestimation since the evaluation of the diagrams involve large sums of terms of different signs. A comparison of double versus single (or quadruple) precision for a range of I can be used to derive a more realistic I -dependent ϵ . (In our particular case we estimated a growth $\propto I^3$ for most contributions).

For the extrapolation we assume an asymptotic expansion in functions $\{f_k(I), k = 1, 2, \dots, n_f\}$ where successive terms become “smaller” with increasing index k ,

$$F(I) = \sum_{k=1}^{n_f} \alpha_k f_k(I) + R(I), \quad (\text{D.2})$$

where $|R(I)/f_{n_f}| \rightarrow 0$ as $I \rightarrow \infty$. Of course, we have in mind something like $\{f_1(I), f_2(I), \dots\} = 1, \ln I/I, \dots, \ln^\mu I/I^\nu, \dots\}$. Denoting the n data values for $F(I)$ as an n -dimensional column vector, the above equation reads

$$F = f\alpha + R, \quad (\text{D.3})$$

where f (evaluated for the n values of I for which we have data) is regarded as an $n \times n_f$ matrix and α is an n_f -dimensional column vector that we want to determine.

In ref. [36] a recursive blocking technique was proposed to determine α which was claimed superior to making least square fits. In the following we shall find that blocking can actually be considered as a particular way of fitting with generalizations however being potentially more convenient.

We determine α by minimizing a quadratic form in the residues

$$\chi^2 = (F - f\alpha)^T W^2 (F - f\alpha). \quad (\text{D.4})$$

Here W^2 is an n -dimensional matrix of positive weights. It can be used to emphasize residues at small or large I in the minimization. Small I are less affected by roundoff, leading to less roundoff errors induced in α . On the other hand for larger I the asymptotic expansion holds to a better degree, and hence here smaller systematic errors are expected. In fact for our data we found little advantage in setting $W_{IJ} = \delta_{IJ} I^z$, $-3 \leq z \leq 3$; and thus we finally used a flat weight $W = 1$ and just changed the I range analyzed to observe convergence by moving I_{\min} while always keeping I_{\max} at the highest available size. The freedom in choice of W could however be useful in different situations and hence we keep it general in the following discussion.

Minimization of (D.4) leads to the equation

$$f^T W^2 f \alpha = f^T W^2 F. \quad (\text{D.5})$$

We assume that the columns of Wf are linearly independent thus spanning an n_f -dimensional subspace ($n_f < n$ must always hold). Let P be the projector on to this subspace. Then

$$Wf\alpha = PWF, \quad (\text{D.6})$$

is an equivalent equation that fixes α . A very stable and convenient way to solve for α is to construct the *singular value decomposition* for Wf [37]. In a very simple version it amounts to a factorization

$$Wf = USV^T, \quad (\text{D.7})$$

where U is a column-orthonormal $n \times n_f$ matrix obeying

$$U^T U = 1; \quad U U^T = P, \quad (\text{D.8})$$

S is diagonal and V orthonormal, both of size $n_f \times n_f$. Then we get

$$\alpha = V S^{-1} U^T W F. \quad (\text{D.9})$$

By simple error propagation the roundoff error of α is

$$\delta_{\alpha_k}^2 = \sum_I (V S^{-1} U^T)_{kI}^2 \delta_{F(I)}^2. \quad (\text{D.10})$$

A simple property of (D.6) is the following. Imagine changing F by a component proportional to one of the functions f_k included in the fit. Then it is easy to see that only the corresponding α_k changes. In other words an estimate of α_1 from (D.9) is only uncertain due to components beyond f_1, \dots, f_{n_f} contained in F . Then it is clear that if we choose the I -window minimal ($n = n_f$ successive values) the solution is equivalent to a blocking procedure cancelling $n_f - 1$ components to isolate say α_1 .

The estimation of the systematic errors is the most delicate problem in our context. After considerable experimentation we propose the following procedure. We assume that the remainder R can be modelled by a linear combination of the n_r functions $f_{n_f+1}, f_{n_f+2}, \dots, f_{n_f+n_r}$ following those included in the fit. Typically in our case these would be the $n_r = 3$ functions $\ln^2 I/I^m, \ln I/I^m, 1/I^m$, if $O(1/I^{m-1})$ is the last order in the fit. If they could be fitted individually (that is distinguished), they would be included in the analysis. Instead, for our error analysis we make n_r separate fits including *only one of them* per fit in addition to the $f_i, i = 1, \dots, n_f$. In this way we get the coefficients A_1, \dots, A_{n_r} of the extra term in each case. The model remainders $A_1 f_{n_f+1}, A_2 f_{n_f+2}, \dots, A_{n_r} f_{n_f+n_r}$ are fitted in the same way as the data (D.9), and the maximal fit-coefficient of the n_r cases is taken as the systematic error d_{α_k} of α_k .

We found that these errors based on the leading *unincluded* contribution are smaller in most (but not all) cases compared to the previous method focussing on the last *included* term. The present errors seem more realistic in the sense that expected relations (like coefficients of the β -function) hold to an accuracy still conservatively but not grossly more accurate than the estimated errors.

References

- [1] M. Lüscher, *Advanced Lattice QCD*, Lectures given at Les Houches Summer School 1997, hep-lat/9802029.
- [2] R. Sommer *Non-perturbative renormalization of QCD* Lectures given at 36. Internationale Universitätswochen für Kern- und Teilchenphysik, Schladming 1997, hep-ph/9711243.
- [3] P. Weisz, Nucl. Phys. B (Proc.Suppl.) 47 (1996) 71.
- [4] S. Capitani, M. Lüscher, R. Sommer and H. Wittig, Nucl. Phys. B544 (1999) 669.
- [5] J. Rolf and U. Wolff, hep-lat/9907007
- [6] S. Capitani et al. (ALPHA collaboration), Nucl. Phys. B (Proc. Suppl.) 63 (1998) 153.
- [7] M. Lüscher, R. Narayanan, P. Weisz and U. Wolff, Nucl. Phys. B384 (1992) 168.
- [8] M. Lüscher, R. Sommer, P. Weisz and U. Wolff, Nucl. Phys. B 413 (1994) 481.
- [9] M. Lüscher and P. Weisz, Phys. Lett. B349 (1995) 165.
- [10] C. Christou, H. Panagopoulos, A. Feo and E. Vicari, Phys. Lett. B426 (1998) 121.
- [11] C. Christou, A. Feo, H. Panagopoulos and E. Vicari, Nucl. Phys. B525 (1998) 387 and Erratum, to be published, see hep-lat/9801007v2
- [12] A. Bode, Nucl. Phys. B (Proc.Suppl.) 63 (1998) 796.
- [13] A. Bode, PhD thesis (in German), Humboldt University, August 1998, <http://dohost.rz.hu-berlin.de/dissertationen/physik/>
- [14] A. Bode, U. Wolff and P. Weisz, Nucl. Phys. B540 (1999) 491.
- [15] B. Sheikholeslami and R. Wohlert, Nucl. Phys. B259 (1992) 168.
- [16] A. Bode, U. Wolff and P. Weisz, hep-lat/9908044.

- [17] S. Sint and R. Sommer, Nucl. Phys. B465 (1996) 71.
- [18] M. Lüscher, S. Sint, R. Sommer, P. Weisz and U. Wolff, Nucl. Phys. B491 (1997) 323
- [19] R. G. Edwards, U. M. Heller and T. R. Klassen, hep-lat/9710054.
- [20] R. Sommer and K. Jansen, Nucl. Phys. B530 (1998) 185
- [21] J. Stehr and P.H. Weisz, Lett.Nuovo Cim.37 (1983) 173.
- [22] A. Gonzalez Arroyo, F.J. Indurain and G. Martinelli, Phys. Lett B117 (1982) 437.
- [23] R. Groot, J. Hoek and J. Smit, Nucl. Phys. B237 (1984) 111.
- [24] R. Wohlert, Improved continuum limit lattice action for quarks, DESY preprint 87-069 (1987) unpublished.
- [25] M. Lüscher and P. Weisz, Nucl. Phys. B479 (1996) 429.
- [26] R. Narayanan and U. Wolff, Nucl. Phys. B444 (1995) 425.
- [27] S. Sint and P. Weisz, Nucl. Phys. B502 (1997) 251.
- [28] H. Panagopoulos, work in progress, private communication.
- [29] S. Sint, private notes (1996).
- [30] G. Marinelli and C. Sachrajda, hep-lat/9812001.
- [31] H. Kawai, R. Nakayama and K. Seo, Nucl. Phys. B189 (1981) 40.
- [32] P. Weisz, Phys. Lett. B100 (1981) 331.
- [33] S. Capitani and G. Rossi, Nucl. Phys. B433 (1995) 351.
- [34] G. de Divitiis, R. Frezzotti, M. Guagnelli, M. Luescher, R. Petronzio, R. Sommer, P. Weisz and U. Wolff, Nucl. Phys. B437 (1995) 447.
- [35] O. V. Tarasov, A. A. Vladimirov and A. Yu. Zharkov, Phys. Lett. B93 (1980) 429.
- [36] M. Lüscher and P. Weisz, Nucl. Phys. B266 (1986) 309.

- [37] W. H. Press, S. A. Teukolsky, W. T. Vetterling, B. P. Flannery. *Numerical recipes: The art of scientific computing*, Univ. Press